Moment Closures for Fusion Optimization

Akash Shukla

April 26, 2020

Contents

Abstract

Turbulent heat loss in a fusion reactor limits its ability to confine heat and produce fusion energy. Exploring tokamak parameters to find configurations that minimize turbulent transport will help us optimize fusion reactors. However, exploring efficiently and accurately is a challenge. Gyrokinetic models can accurately calculate turbulence but are too expensive to explore a broad parameter space with. Gyrofluid models are cheap, but they rely on moment closures that break down in the presence of turbulence. In order to develop a fast and accurate model to explore with, we will need robust closures that correctly capture nonlinear kinetic effects.

As a starting point, we have developed such a closure for a simplified nonlinear gyrokinetic system, DNA (Hatch et al.), which models ITG turbulence in an unsheared slab. Numerical tests in the DNA simulation show that out new Dynami Multi-Mode (DMM) closure outperforms standard closures and extrapolates to different parameter regimes.

1 Background

1.1 Plasma Turbulence

Fusion plasmas are inherently turbulent. Plasma turbulence covers a wide range of spatial and temporal scales - the smallest turbulent fluctuations are on the scale of the ion Larmor radius (ρ_i), while the bulk properties of the plasma, which contain the gradients that cause these small fluctuations, occur on the scale of the device (maybe the radius of the tokamak.) These bulk properties, the mean fields, fluctuate at a rate $1/\tau_E$, where τ_E is the confinement time, that is many (10^3) times slower than the turbulent fluctuation frequency, ω [1].

The presence of relevant physical processes on such disparate scales and the non-local nature of the electromagnetic interactions in the plasma make modeling the dynamics very complex and computationally expensive. Fortunately, we have been able to take advantage of the large separation between the small scales of the turbulent fluctuations and the large scales of the variation of the mean fields which cause them, building reduced models which average over the small time and space scales and track only the slow evolution of the bulk properties of interest[2].

1.2 Plasma Modeling

A kinetic description of a plasma defines the evolution of the distribution function for particles at position $\vec{x}$ and velocity $\vec{v}$ in time according to the Boltzmann Equation:

$$\frac{\partial f_s}{\partial t} + \boldsymbol{v} \cdot \nabla f_s + \frac{q}{m}\left(\boldsymbol{E} + \frac{\boldsymbol{v}}{c} \times \boldsymbol{B}\right) \cdot \nabla_v f = C[f_s], \tag{1}$$

where $f_s(\boldsymbol{x}, \boldsymbol{v})$ denotes the distribution function of particle species s, $\boldsymbol{E}$ is the electric field, $\boldsymbol{B}$ is the magnetic field, and C is a collision operator. In order to calculate the self-consistent fields, this must be coupled to Maxwell's equations. The kinetic equation time-evolves a six dimensional phase space at the fast cyclotron frequency rendering it extremely challenging to solve numerically. Although direct numerical simulations of Eq. 1 can be achieved at great expense for limited problems, the the full kinetic equation remains, perhaps, most valuable as a starting point for reduced treatments of plasmas.

One of these reduced treatments, gyrokinetics, has proven to be an extremely useful description of plasmas in strongly magnetized regimes [3, 4]. The gyrokinetic model averages out the fast gyration of the particles around the magnetic field, reducing the distribution function from 6D to 5D (3 spatial dimensions and 2 velocity dimensions) and eliminating the fast cyclotron timescale, drastically reducing the cost of simulations. The gyrokinetic equation effectively evolves a distribution of 'charged rings', and is expressed in terms of the guiding center coordinates and gyro-averaged fields.

Gyrokinetics has become the standard tool for describing turbulent transport in magnetic fusion devices, and more broadly, has found fruitful applications ranging from basic plasma physics to space / astro systems [5, 6, 7, 8]. In fusion applications, in particular, gyrokinetics has demonstrated ever increasing explanatory power and fidelity with respect to experimental observations [9, 10, 11]. Despite these developments, nonlinear gyrokinetics remains too expensive to be routinely used to predict confinement (i.e., to evolve profiles) or broadly explore parameter space for optimal confinement configurations. Consequently, further reductions in complexity remain highly desirable.

One such approach to further reducing the gyrokinetic system, the gyrofluid framework, was vigorously explored in the 90s [12, 13]. A critical component of gyrofluid models is closures that capture important kinetic effects within the fluid framework. A prototypical example is the Hammett and Perkins (HP)[12] closure, which closes a fluid system in collisionless regimes using the linear kinetic response. The HP closure is much more rigorous for collisionless plasmas than conventional fluid closures, faithfully reproducing kinetic effects (i.e., phase mixing / Landau damping) and resulting in linear growth rates and frequencies in quite good agreement with the true (kinetic) values. However, its validity is not well established in systems outside its targeted collisionless parameter regime nor in turbulent systems where nonlinear mixing can alter phase mixing dynamics [14, 15, 16, 17]. In effect, the standard gyrofluid closures hard-wire the linear physics into the closure, eliminating potentially important nonlinear modifications to the physics.

1.3 Gyrokinetics

In order to obtain the gyrokinetic equation from the kinetic, the fast 'gyromotion', the gyration of the ions around the magnetic field at the larmor frequency, must be removed in order to reduce the number of velocity dimensions from three to two. This reduction also necessitates a change of perspective; we are no longer describing the motion of charged particles, but that of charged rings centered at the *gyro-center*.

To do so, we first transform into the guiding-center or 'drift' coordinates. The gyro-center $\vec{R}$ is defined in terms of the particle position $\vec{r}$ and particle velocity $\vec{v}$

$$\vec{R} = \vec{r} + \frac{\vec{v} \times \vec{b}_0}{\Omega_0} \tag{2}$$

where $b_0 = b_0(\vec{r}) = B_0/B_0$ is the unit vector along the local equilibrium field and $\Omega_0 = \Omega_0(\vec{r}) = qB_0/m$. The parallel andperpendicular velocity, $v_|$| and $v_\perp$, and the gyro-angle, θ with respect to the equilibrium magnetic field (b_0) are defined by the expression:

$$\vec{v} = v_{||}\vec{b}_0 + v_\perp(\cos\theta\vec{e}_1 + \sin\theta\vec{e}_2)$$

The unit vectors $\vec{b}_0, \vec{e}_1,$ and $\vec{e}_2$ form a local right handed coordinate basis i.e. $\vec{e}_1 \times \vec{e}_2 = \vec{b}_0$, and

they vary on the macroscopic, L, spacial scale and the slow, τ, time scale. In the straight field (electrostatic) case, $\vec{b_0} = \hat{z}, \vec{e}1 = \hat{x}$ and $\vec{e}_2 = \hat{y}$.

The fastest motion is the gyromotion ($\frac{d\theta}{dt}$). This is the motion over which we need to average. The average we take, the *gyro-average* (ring-average) is defined in our new coordinate system as follows:

$$< a(\vec{r}, \vec{v}, t) >_R = \frac{1}{2\pi} \int_0^{2\pi} a(\vec{R} - \frac{\vec{v} \times b_0}{\Omega_0}, \vec{v}, t) d\theta.$$

This integration over θ is done at constant $\vec{R}$, $\vec{v}_\perp$, and$v_{||}$. So, the gyro-average is an average over a ring centered at $\vec{R}$ of radius $\vec{v}_\perp/\Omega_0$. By separating the components of the kinetic ion-fokker planck equation into their respective length and time scales based on the small parameter $\epsilon = \frac{\rho}{L}$ and gyro-averaging these separated Equations, we have, at order ϵ, the gyrokinetic equation:

$$\frac{\partial h}{\partial t} + v_{||} \frac{\partial h}{\partial Z} + \vec{v}_D \cdot \frac{\partial h}{\partial \vec{R}} - \frac{\partial \phi}{\partial \vec{R}} \times (\frac{\vec{b}_0}{B_0}) \cdot \frac{\partial h}{\partial R} - \left\langle \tilde{C}(h) \right\rangle = q \frac{F_0}{T_0} \frac{\partial < \phi >}{\partial \vec{R}} \times (\frac{\vec{b}_0}{B_0}) \cdot \frac{\partial F_0}{\partial \vec{R}}$$

and

$$\vec{v}_D = -\frac{v_\perp^2}{2\Omega_0} \frac{\boldsymbol{\nabla} B_0}{B_0} \times \vec{b}_0 = \frac{v_\perp^2}{2B_0} \frac{1}{\Omega_0} \frac{dB_0}{dx} \vec{y}$$

The gyrokinetic description is very similar to the kinetic description and retains much of the accuracy of the kinetic description; it is still able to describe the small scale turbulent fluctuations at the medium frequency, ω.

1.4 Fluid & Gyrofluid Models

The fluid description focuses on the mean fields and velocity moments of the plasma. The n$^t h$ velocity moment of the plasma distributon function can be obtained by integrating the kinetic distribution function multiplied by velocity raised to the nth power with respect to velocity:

$$f(\vec{x}, \vec{v}, t)$$

$$n(\vec{x}, t) = \int f(\vec{x}, \vec{v}, t) d\vec{v} \rightarrow \rho = \sum qn$$

$$u(\vec{x}, t) = \int \vec{v} f(\vec{x}, \vec{v}, t) d\vec{v} \rightarrow \vec{J} = \sum qu$$

$$P(\vec{x}, t) = \frac{m}{3} \int v^2 f(\vec{x}, \vec{v}, t) d\vec{v}$$

where n = density, u = mean velocity, p is pressure, q = heat flux, moments r and up aren't physically meaningful.

Gyrofluid models are similar to fluid models, the only difference being that they are derived from the gyrokinetic instead of kinetic equation. The gyrofluid equations are obtained by taking moments of the gyrokinetic equation with respect to velocity; multiplying the gyrokinetic equation

by velocity raised to the nth power and then integrating with respect to velocity gives the evolution equation for the nth moment. The first few moment equations are shown below:

$$\frac{\partial n}{\partial t} + n_0 \frac{\partial u}{\partial z} = 0 \tag{3}$$

$$\frac{\partial u}{\partial t} + \frac{1}{mn_0}\frac{\partial p}{\partial z} - \frac{eE}{m} n_0 = 0 \tag{4}$$

$$\frac{\partial p}{\partial t} + \frac{\partial q}{\partial z} + 3p_0 \frac{\partial u}{\partial z} = 0 \tag{5}$$

$$\frac{\partial q}{\partial t} + \frac{\partial uq}{\partial z} + 3q\frac{\partial u}{\partial z} - \frac{3p}{mn}\frac{\partial p}{\partial z} - \frac{\partial r}{\partial z} = 0 \tag{6}$$

1.5 Moment Closures

Note that in Eq 3, the evolution equation for each moment depends on the next higher moment. This is what gives rise to the closure problem; the evolution of a givenmoment depends directly on the next higher or-der moment, so the set of equations is not closed. Some approximation scheme for the highest moment, a moment closure, is required.

The most widely used closure for the gyrofluid system described in Eq 3, the HP closure, expresses the 4th moment (r) in terms of the heat flux (q), pressure (p), and density (n) fluctuatons, proposing a closure of the form:

$$r = Ai\frac{k_\parallel}{|k_\parallel|}q + B(p - T_0 n). \tag{7}$$

Choosing coefficients A and B so that the fluid response resulting from the combination of the closure ansatz 7 and the gyrofluid equations 3 matches the linear kinetic response in the low and high frequency limits results in the HP Closure.

Below, we describe comparisons between three closure schemes: (1) HP, (2) simple truncation, and (3) our novel SVD-based closure.

2 Results

2.1 The DNA Code

In order to explore various closure ideas, we study a relatively simple kinetic turbulent system—ITG / ETG instability and turbulence in an unsheared slab. The underlying model is a reduction of gyrokinetics to one dimension (parallel to the magnetic field) in velocity space and retaining rudimentary finite Larmor radius (FLR) effects of the form $e^{-k_\perp^2 \rho_s^2}$. The parallel velocity dimension is then decomposed on a basis of Hermite polynomials, resulting in the following set of equations [18, 19].

$$\frac{\partial g_n}{\partial t} = L[g_n] + N[g_n] \tag{8}$$

with the following linear and nonlinear operators:

$$\begin{aligned} L[g_n] =& \omega_T i k_y \frac{k_\perp^2}{2} e^{k_\perp^2/2} \phi \delta_{n,0} - \omega_n i k_y e^{k_\perp^2/2} \phi \delta_{n,0} \\ & - \omega_T i k_y e^{k_\perp^2/2} \phi \delta_{n,2} - i k_z e^{k_\perp^2/2} \phi \delta_{n,1} \\ & - i k_z [\sqrt{n} g_{n-1} + \sqrt{n+1} g_{n+1}] - \nu n g_n \end{aligned} \tag{9}$$

$$N[g] = \sum_{\vec{k}'} (k_x' k_y - k_x k_y') e^{-k_\perp'^2/2} \phi_{\vec{k}'} g_{\vec{k}-\vec{k}'} \tag{10}$$

where

$$\phi = \frac{e^{-k_\perp^2} g_0}{1 + \tau - \Gamma_0(k_\perp^2)}, \tag{11}$$

ω_T is the normalized inverse temperature gradient scale length, ω_n is the normalized inverse density gradient scale length, ν is the collision frequency, and n is the number of the Hermite moment. The wavenumbers $k_{x,y,z}$ are in the direction of the background gradients, binormal direction, and parallel (to the magnetic field) direction, respectively. This system of equations is numerically solved using the DNA code [18, 19].

The phase mixing term, $ik_z[\sqrt{n} g_{n-1} + \sqrt{n+1} g_{n+1}]$, depends on $g_{n\pm1}$ and results in the transfer of energy between scales in phase space. The dependence of the equation for g_n on g_{n+1} is responsible for the closure problem; the evolution of a given moment depends directly on the next higher order moment, so the set of equations is not closed. Some approximation scheme is required. The simplest closure scheme is truncation: explicitly evolve $n_{\max}$ moment equations, and set $g_{n_{\max}+1} = 0$. If a sufficiently high number of moments are retained, the simulation can be considered to be kinetic and closure by truncation generally does not disturb the low order moments. If, however, one wishes to evolve a fluid system (i.e. evolve only a few moments), simple truncation will generally produce deviations from the kinetic system, particularly at low collisionality where Landau damping / phase mixing is an important effect.

2.2 Limitations of the HP Closure

The HP closure has been shown to faithfully reproduce kinetic Landau damping rates and linear growth rates. Indeed, our simulations exhibit good agreement between kinetic linear growth rates and fluid growth rates using the HP closure. A representative example is shown in Fig. 1, where it is seen that the HP closure and the full kinetic system produce unstable growth rates that are in close agreement

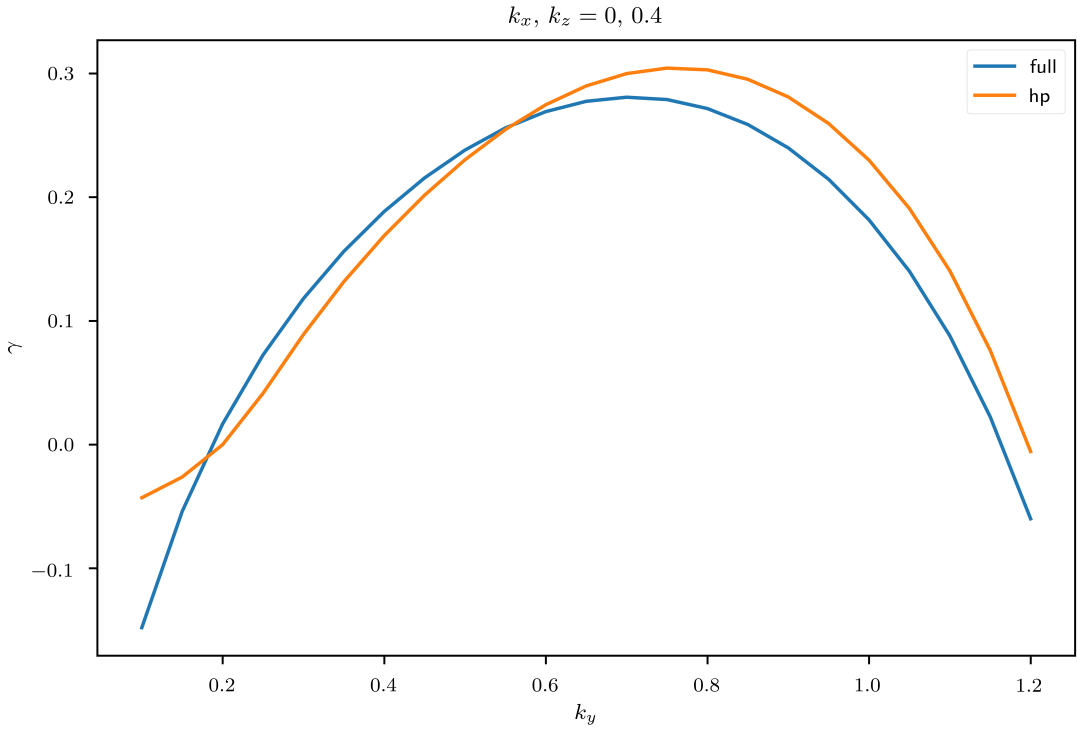

Figure 1: Linear growth rates (γ) produced by eigenvalue calculations using the fluid model with the HP closure and the fully kinetic model at the most unstable wavenumber, k_x, k_y, k_z = 0, 0.7, 0.4, for temperature gradient drive (ω_T) = 8, collision frequency (ν) = 0.05.

However, the focus solely on linear physics is a major limitation. Several recent papers have shown that Landau damping or phase mixing rates in the presence of turbulence can differ substantially from the linear expectation [14, 15, 16, 17]. If one constructs the energy equation corresponding to Eqs, 9 10, the contribution from phase mixing defines the energy flux to higher order moments [19]: $J_{n+1/2} = \pi^{1/2} i k_z \sqrt{n+1} g_n^* g_{n+1}$. In words, the rate at which energy is transferred to/from higher order moments is defined by a correlation between two neighboring moments. The linear physics defines a fixed relationship between g_n and g_{n+1}, which the HP closure hard-codes into the model. In the presence of turbulence, however, the various moments are continually perturbed by the nonlinearity, resulting in correlations that can differ substantially from the linear expectation.

In order to gain insight into these dynamics, we analyze the simulated values of the coefficients governing the relationship between g_4 and g_3 (A) as well as g_4 and g_2 (B). Simulation data from the the most unstable wavenumber, k_x, k_y, k_z = 0, 0.7, 0.4, is shown in Fig. 2 for parameter point ($\omega_T = 8, \nu = 0.05$), at which both HP and simple truncation deviate strongly from a kinetic simulation. The figure shows the coefficients in the nonlinear simulation along with the HP values.

The coefficients in the nonlinear simulation exhibit a broad distribution of values (shown in the pdf in the upper panels) with a peak that does not correspond to the HP value. Moreover, the coefficients vary rapidly in time and oscillate between positive and negative values, suggesting that a closure would benefit from the versatility to allow for energy transfer both to *and* from higher order moments. The HP closure is strictly dissipative, which is likely a major reason for its inaccuracies in the nonlinear turbulence, as described below.

We note the connections between this closure and the line of research exploring the role of damped eigenmodes in plasma micro turbulence [20, 21, 16, 22], which clearly shows that subdominant stable modes play a crucial role in the turbulent energetics. We note also, the closure defined in Ref. [23, 24], which appeals to both the ITG instability and its complex conjugate mode in formulating the closure. Although that closure is static (i.e. constant in time), it clearly demonstrates the need for the advantages of allowing energy transfer both to and from higher order moments. These observations support our premise that a suitable closure in a nonlinear system may require more flexibility than is allowed by a static, constant coefficient closure.

2.3 SVD Closure

Motivated by the results in the previous section, here we seek a dynamic, flexible closure for phase mixing in a turbulent system. More specifically, we seek to accurately resolve the low-order moments, $g_{0:3}$ that define the physical quantities of interest and determine transport fluxes, without retaining the higher order moments $g_{4:\infty}$.

The proposed method requires a single kinetic simulation to formulate a set of basis vectors. In our case, we use 48 Hermite moments for the full kinetic simulation. Any number of subsequent fast / fluid simulations can then be run requiring explicit computation of only $g_{0:3}$.

The full kinetic simulation is used as follows. Let $G_{N\times M}$ (M is the number of time points and N is number of moments retained in the fluid model plus one) be the matrix created from the simulated distribution function at a single wave vector $g_n(t)$ so that $G_{ij} = g_i(t_j)$:

$$G = \begin{bmatrix} g_0(t_0) & g_0(t_1) & \cdots & g_0(t_M) \\ g_1(t_0) & g_1(t_1) & \cdots & g_1(t_M) \\ g_2(t_0) & g_2(t_1) & \cdots & g_2(t_M) \\ g_3(t_0) & g_3(t_1) & \cdots & g_3(t_M) \\ g_4(t_0) & g_4(t_1) & \cdots & g_4(t_M) \end{bmatrix} \tag{12}$$

The SVD of G is given by

$$G_{N\times M} = U_{N\times N}\Sigma_{N\times N}V^H_{N\times M} \tag{13}$$

where U and V are unitary and Σ is diagonal with real entries. The columns of the matrix U are

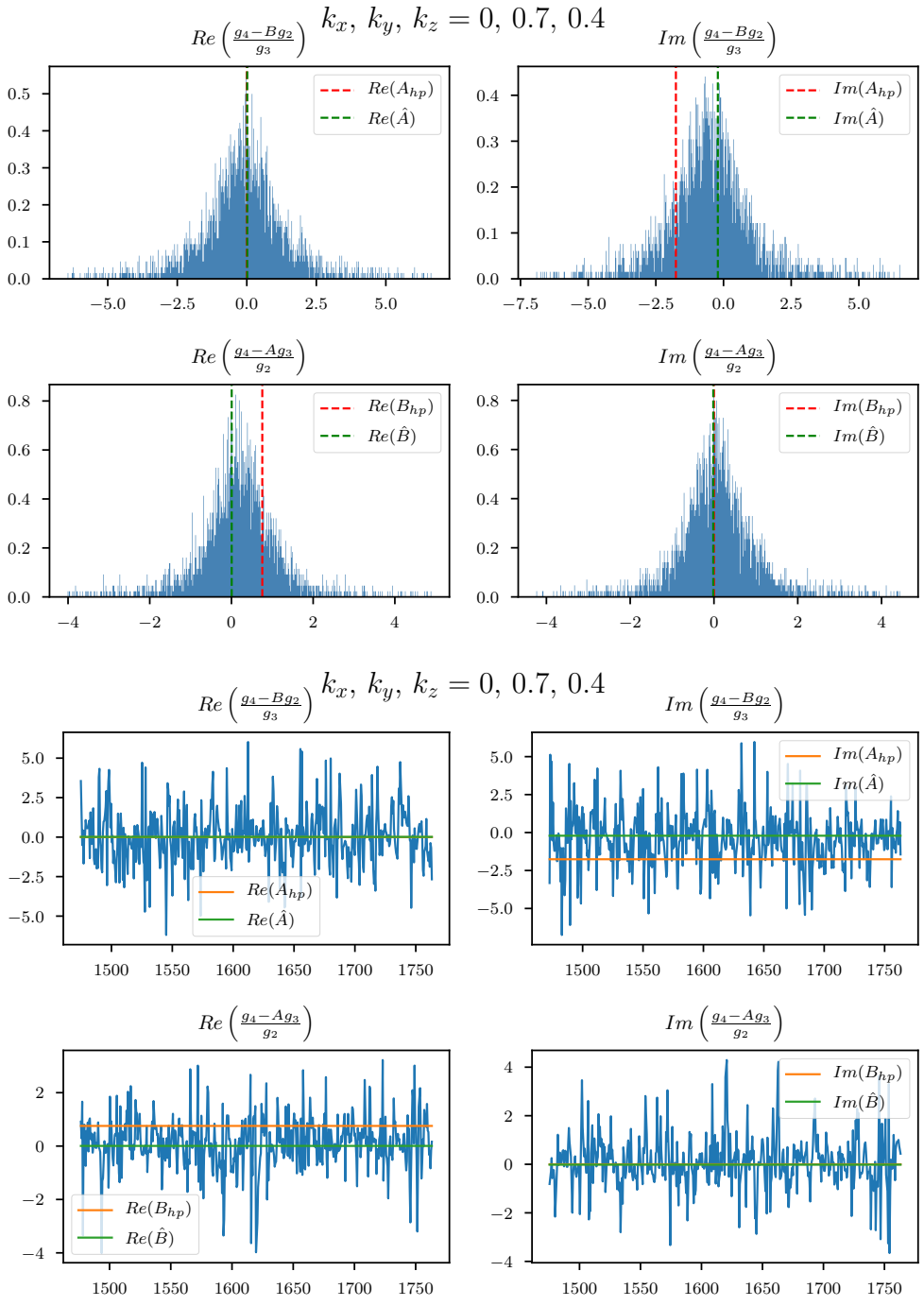

Figure 2: Coefficients relating g_4 and g_3 (A) and g_4 and g_2 (B) from a simulation at parameter point $\omega_T = 8, \nu = 0.05$ are shown at the most unstable wavenumber, $k_x,\ k_y,\ k_z = 0,\ 0.7,\ 0.4$. The HP coefficients are not at the centers of the distributions marked by $\hat{A}$ and $\hat{B}$. The oscillation of the coefficients from the simulation in time suggests that a closure should not be strictly dissipative and that the closure relationship is time dependent.

the N strongest eigenmodes and the rows of ΣV^H are the time traces of the amplitude of each of these eigenmodes.

For the purposes of our desired four moment model, we select $N = 5$ (i.e. only a small subset of the 48 total Hermite moments), which is sufficient to fully exploit the information in the simulation defining the natural (kinetic, turbulent) relations between g_3 and g_4.

In each time step of a subsequent fluid simulation, we numerically advance $g_{0:3}$ explicitly. The truncated moment, g_4, is calculated as follows. First, we project the state vector $g0:3$ onto the basis formed by the columns of U. This entails finding the projection coefficients that define the amount of each SVD mode in the turbulent state at a given point in time. We will call these projection coefficients $\hat{v}$. We can do this by removing the row corresponding to the unknown N^{th} moment from U and extracting $\hat{v}$ from the following equation:

$$g_{0:3} = U_{0:3,0:4}\hat{v} \tag{14}$$

This gives

$$\hat{v} = (U_{0:3,0:4})^{\dagger} g_{0:3} \tag{15}$$

where † denotes the pseudo-inverse.

Now that we have $\hat{v}$, a length N vector of the inferred mode strengths, we can predict $\hat{g}_4$ by applying these mode strengths to the previously removed row of U, $U[4,:]$. This gives

$$\hat{g}_4 = U[4,:]\hat{v} = U_{4,0:4}(U_{0:3,0:4})^{\dagger} g_{0:3} \tag{16}$$

This procedure results in a closure that has the same number of degrees of freedom as the underlying fluid model and can dynamically adapt to the nonlinear state of the system.

Moreover, although some extra computational expense is required by the projection, this is on the order of the other terms in the linear operator and much less demanding than the pseudo-spectral computation of the nonlinearity. In fact, the projection is only slightly more expensive than the HP closure. The HP closure requires 2 complex multiplications ($A \cdot g_3$ and $B * g_2$) per wave vector (k) per time step. The DMM closure amounts to a dot product between two length 4 vectors because in Eq. 16, $U_{4,0:4}(U^{\dagger}_{0:3,0:4})$ is a 1x4 vector times a 5 by 4 matrix which results in a 1x4 vector. This product is computed ahead of time and saved to a file which is loaded at the beginning of the simulation. In the simulation, this 1x4 vector must be dotted with $g_{0:3}$, which is a 4x1 vector to get the closure for g_4. Thus, the DMM closure requires 4 complex multiplications per wave vector per time step.

2.4 Simulation Results

DNA simulations covering a wide range of temperature gradients, ω_T, and collision frequencies, ν, were conducted with a fully (reduced gyro-) kinetic model (48 moments), simply truncated model

(4 moments, 5^{th} is set to 0), the DMM closure, and the standard Hammett-Perkins (HP) closure for the 4^{th} moment.

The exact HP closure used was $g_4 = 0.754860 g_2 - i(1.759312 sgn(k_z)) g_3$. The matrix of basis vectors, U, for the DMM closure was obtained from a full 48 moment simulation with parameters $\omega_T = 6$ and $\nu = 0.01$. The scan covers $\omega_T = 5, 6, 7, 8, 9$, and $\nu = 0.01, 0.05, 0.1, 0.2$.

Ultimately, we would like closed simulations to reproduce the macroscopic behavior of gyrokinetic simulations, so the performance of the closures was evaluated primarily by comparing the saturated value of the total radial heat flux, Q, to that of the full simulation.

Time traces of the heat flux produced by all four types of simulation are shown for each combination of input parameters, ω_T and ν, in Fig. 3.

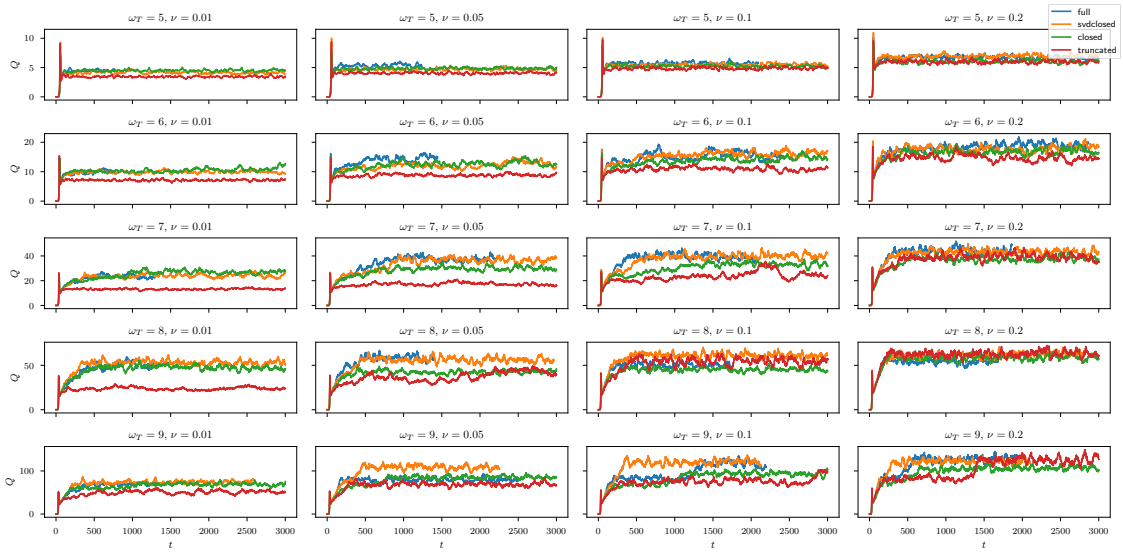

Figure 3: Time traces of the perpendicular heat flux (Q) for full (blue), hp-closed (green), svd-closed (orange), and truncated (red) simulations for temperature gradient drives (ω_T) ranging from 5 to 9 (increasing downward by panel) and collision frequencies (ν) ranging from 0.01 to 0.2 (increasing to the right by panel). The metric of performance is the final saturation level. The HP closure performs well at low collisionality but deteriorates, predicting a too-low saturation level, as collisionality increases. The DMM closure generally shows better performance than both the HP closure and truncation.

The simplest metric for the performance of the closure is the proximity of the saturated heat flux for a given closure scheme to that of the full kinetic simulation. The final saturation levels of each simulation type at each set of input parameters were calculated by averaging over the last half of the time trace. Each plot in Fig. 4 shows the percent error in saturated heat flux, $(Q^{closed} - Q_{full})/Q_{full}$, for all parameter combinations for each closure scheme.

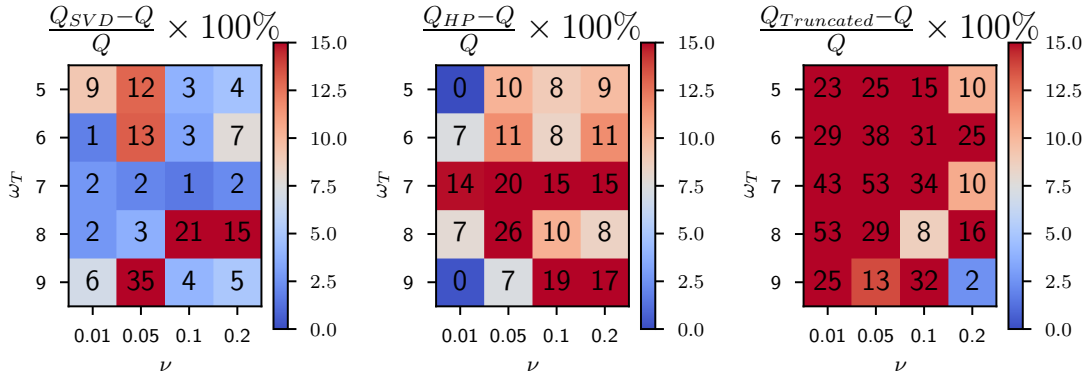

Figure 4: Percent error in saturated heat flux for each closure (lef: SVD, middle: HP, right: truncation) as compared against the full simulation for temperature gradient drives (ω_T) ranging from 5 to 9 (increasing downward) and collision frequencies (ν) ranging from 0.01 to 0.2 (increasing to the right). The basis of singular vectors was extracted from the $\omega_T = 6$, $\nu = 0.01$ simulation, but the DMM closure's performance does not appear to systematically deteriorate as simulations move farther from this point in parameter space, indicating that it is robust to changes in input parameters and should be applicable throughout a broader parameter space.

As expected, simple truncation performs poorly compared to the other two closures with errors roughly ranging from $20 - 50\%$. Note however, that the truncation errors are smallest at the highest value of collisionality, suggesting that as collisionality increases the simple fluid treatment becomes more accurate, thus confirming the expectation for a fluid treatment.

The HP closure works well in the low collisionality regime for which it was designed (note the small errors at $\nu = 0.01$). However, its performance deteriorates as collisionality is increased. The HP errors are also larger as the gradient drive increases and the phase mixing physics must compete with ω_* physics and the nonlinearlity. This suggests that the HP closure is well-suited for the its targeted regime (a regime where phase mixing dominates). However, when other physics enters (strong gradient drive, nonlinearity, and/or collisions), it is too restrictive.

The DMM closure generally shows better performance than both the HP closure and truncation

and, with few exceptions, performs well throughout the parameter space. Although the basis of singular vectors was extracted from the $\omega_T = 6$, $\nu = 0.01$ simulation, its performance does not appear to systematically deteriorate as simulations move farther from this point in parameter space. This indicates that the closure relation in the DMM closure is robust to changes in input parameters and should be more robust throughout a broader parameter space.

In fact, considering the oscillation and range of the coefficients, one may question whether any static closure with fixed coefficients could capture the effects of the kinetic simulation. The DMM closure is dynamic: at each time it determines a new set of 4 coefficients based on mode strengths inferred from the values of the lower moments. This time-dependent closure is very flexible. This flexibility may be the key to effective extrapolation. Perhaps the strength of the closure lies not in the accuracy of the extracted basis vectors, but rather, the capacity to adapt dynamically to the nonlinear state. These ideas will be explored further in future work.

3 Discussion

We have compared several closure methods for a relatively simple turbulent system—ITG/ETG driven turbulence in an unsheared slab—throughout the relevant 2D parameter space (collisionality and gradient drive). Comparisons between four-moment fluid systems and a kinetic treatment demonstrate that simple truncation performs poorly, with errors roughly at the level of $20 - 50\%$, while the HP closure performs much better, particularly in the low collisionality regime. Our new DMM closure outperforms both throughout the parameter space with errors generally less than 10%. The DMM closure has the advantage of dynamically allowing the closure coefficients to vary in time depending on the details of the nonlinear turbulent state. Consequently, the approach appears to be much more robust throughout a broader parameter space and, in particular, in the presence of turbulence.

This approach can potentially be generalized/adapted in several ways. For example, basis vectors could be periodically enriched by performing kinetic simulations sparsely throughout parameter space. Additionally, suitable basis vectors could potentially be formulated without the need for a nonlinear kinetic simulation by, e.g., taking inspiration from linear eigenmodes or otherwise using physics-based intuition. We also note that the closure coefficients tend to center around 0, as shown in Fig. 2, suggesting that a deeper look at the raw statistics of the closure may prove fruitful.

Moreover, although this method was tested here in a simple system, the approach can be easily generalized to a more comprehensive toroidal system (e.g. that described in Ref. [25]) and, potentially, to other closure problems (e.g. curvature terms, FLR effects, etc.). This method could

also be applied to stellarator optimization problems by extending it to the fluid models developed in Ref. [26], which describe the ion temperature gradient turbulent saturation processes in stellarators and also rely on closures.

Integrating this dynamic closure method with realistic simulations of tokamak or stellarator plasmas has great potential for fusion optimization. Fast simulations that accurately reproduce the macroscopic properties of turbulence would make broad exploration of parameter space feasible, enabling parameter exploration and configuration optimization at an unprecedented scale.

References

[1] *Gyro-Kinetics Lectures. From ITER Time-scales to Gyro-Kinetics*, Wolfgang Pauli Institute, 2008.

[2] I. G. Abel, G. G. Plunk, E. Wang, M. Barnes, S. C. Cowley, W. Dorland, and A. A. Schekochihin, "Multiscale gyrokinetics for rotating tokamak plasmas: fluctuations, transport and energy flows," *Reports on Progress in Physics*, vol. 76, p. 116201, oct 2013.

[3] J. A. Krommes, "The gyrokinetic description of microturbulence in magnetized plasmas," *Annual Review of Fluid Mechanics*, vol. 44, no. 1, pp. 175–201, 2012.

[4] E. A. Frieman and L. Chen, "Nonlinear gyrokinetic equations for low frequency electromagnetic waves in general plasma equilibria," *The Physics of Fluids*, vol. 25, no. 3, pp. 502–508, 1982.

[5] G. G. PLUNK, S. C. COWLEY, A. A. SCHEKOCHIHIN, and T. TATSUNO, "Two-dimensional gyrokinetic turbulence," *Journal of Fluid Mechanics*, vol. 664, p. 407–435, 2010.

[6] M. J. Pueschel, F. Jenko, D. Told, and J. Büchner, "Gyrokinetic simulations of magnetic reconnection," *Physics of Plasmas*, vol. 18, no. 11, p. 112102, 2011.

[7] D. Told, F. Jenko, J. M. TenBarge, G. G. Howes, and G. W. Hammett, "Multiscale nature of the dissipation range in gyrokinetic simulations of alfvénic turbulence," *Phys. Rev. Lett.*, vol. 115, p. 025003, Jul 2015.

[8] G. G. Howes, S. C. Cowley, W. Dorland, G. W. Hammett, E. Quataert, and A. A. Schekochihin, "A model of turbulence in magnetized plasmas: Implications for the dissipation range in the solar wind," *Journal of Geophysical Research: Space Physics (1978–2012)*, vol. 113, 5 2008.

[9] T. Görler, A. E. White, D. Told, F. Jenko, C. Holland, and T. L. Rhodes, "A flux-matched gyrokinetic analysis of diii-d l-mode turbulence," *Physics of Plasmas*, vol. 21, no. 12, p. 122307, 2014.

[10] D. Hatch, M. Kotschenreuther, S. Mahajan, P. Valanju, F. Jenko, D. Told, T. Görler, and S. Saarelma, "Microtearing turbulence limiting the JET-ILW pedestal," *Nuclear Fusion*, vol. 56, p. 104003, aug 2016.

[11] C. Holland, "Validation metrics for turbulent plasma transport," *Physics of Plasmas*, vol. 23, no. 6, p. 060901, 2016.

[12] G. W. Hammett and F. W. Perkins, "Fluid moment models for landau damping with application to the ion-temperature-gradient instability," *Phys. Rev. Lett.*, vol. 64, pp. 3019–3022, Jun 1990.

[13] W. Dorland and G. W. Hammett, "Gyrofluid turbulence models with kinetic effects," *Physics of Fluids B: Plasma Physics*, vol. 5, no. 3, pp. 812–835, 1993.

[14] G. G. Plunk, "Landau damping in a turbulent setting," *Physics of Plasmas*, vol. 20, no. 3, p. 032304, 2013.

[15] A. Kanekar, A. A. Schekochihin, W. Dorland, and N. F. Loureiro, "Fluctuation-dissipation relations for a plasma-kinetic langevin equation," *Journal of Plasma Physics*, vol. 81, no. 1, p. 305810104, 2015.

[16] D. R. Hatch, F. Jenko, A. B. Navarro, V. Bratanov, P. W. Terry, and M. J. Pueschel, "Linear signatures in nonlinear gyrokinetics: interpreting turbulence with pseudospectra," *New Journal of Physics*, vol. 18, p. 075018, jul 2016.

[17] R. Meyrand, A. Kanekar, W. Dorland, and A. A. Schekochihin, "Fluidization of collisionless plasma turbulence," *Proceedings of the National Academy of Sciences*, vol. 116, no. 4, pp. 1185–1194, 2019.

[18] D. R. Hatch, F. Jenko, A. Bañón Navarro, and V. Bratanov, "Transition between saturation regimes of gyrokinetic turbulence," *Phys. Rev. Lett.*, vol. 111, p. 175001, Oct 2013.

[19] D. R. Hatch, F. Jenko, V. Bratanov, and A. B. Navarro, "Phase space scales of free energy dissipation in gradient-driven gyrokinetic turbulence," *Journal of Plasma Physics*, vol. 80, no. 4, pp. 531–551, 2014.

[20] P. W. Terry, D. A. Baver, and S. Gupta, "Role of stable eigenmodes in saturated local plasma turbulence," *Physics of Plasmas*, vol. 13, no. 2, p. 022307, 2006.

[21] D. R. Hatch, P. W. Terry, F. Jenko, F. Merz, M. J. Pueschel, W. M. Nevins, and E. Wang, "Role of subdominant stable modes in plasma microturbulence," *Physics of Plasmas*, vol. 18, no. 5, p. 055706, 2011.

[22] G. G. Whelan, M. J. Pueschel, and P. W. Terry, "Nonlinear electromagnetic stabilization of plasma microturbulence," *Phys. Rev. Lett.*, vol. 120, p. 175002, Apr 2018.

[23] H. Sugama, T.-H. Watanabe, and W. Horton, "Collisionless kinetic-fluid closure and its application to the three-mode ion temperature gradient driven system," *Physics of Plasmas*, vol. 8, no. 6, pp. 2617–2628, 2001.

[24] H. Sugama, T.-H. Watanabe, and W. Horton, "Comparison between kinetic and fluid simulations of slab ion temperature gradient driven turbulence," *Physics of Plasmas*, vol. 10, no. 3, pp. 726–736, 2003.

[25] N. R. Mandell, W. Dorland, and M. Landreman, "Laguerre–hermite pseudo-spectral velocity formulation of gyrokinetics," *Journal of Plasma Physics*, vol. 84, no. 1, p. 905840108, 2018.

[26] C. Hegna, P. Terry, and B. Faber, "Theory of itg turbulent saturation in stellarators: Identifying mechanisms to reduce turbulent transport," *Physics of Plasmas*, vol. 25, p. 022511, 02 2018.